RADIATION AND REFRACTION OF SOUND WAVES THROUGH A TWO-DIMENSIONAL SHEAR LAYER

Shi Zheng*, **Steve A. E. Miller**¶, **Mei Zhuang**§
Department of Mechanical Engineering
Michigan State University, East Lansing, MI 48823
Tel: (517)353-9450 Fax: (517)353-1750 Email: zhuangm@egr.msu.edu

ABSTRACT

This report presents solutions to Problem 1 of Category 4 in the 4th CAA Workshop on Benchmark Problems. The problem is numerically solved on a clustered orthogonal grid using a high-order optimized upwind Dispersion-Relation-Preserving scheme. The Perfectly-Matched-Layer (PML) boundary condition in unsplit physical variables is applied to ensure minimum numerical reflections. The numerical results by solving the linearized Euler equations are the total solution, being the superposition of the acoustic wave solution and the instability wave solution. In order to get the instability wave solution, a source term of the same excitation frequency is effectively placed upstream of the region of interest. Such a source term produces a stronger instability wave of the same excitation frequency but a weaker acoustic wave in the region of interest and thus the total solution in this region can well approximate a pure instability wave. The acoustic wave solution, which is desired in the problem, is then successfully achieved by subtracting the instability wave solution from the total solution. The benchmark problem is also analytically solved to an accuracy sufficient to evaluate the numerical solutions.

1. INTRODUCTION

In this paper, we demonstrate an approach of separating the instability waves and the acoustic waves by solving Problem 1 of Category 4 in the 4th CAA Workshop on Benchmark (ref. 1). The formulation of the problem is given in the next section. In section 3, analysis is made to show the existence of the instability wave induced by the acoustic source and the analytical solution is also presented. In section 4, our numerical methodology is described and our approach of numerically separating the instability waves and the acoustic waves is demonstrated. The numerical results are shown in comparison with the analytical solutions. In section 5 are our conclusions.

2. FORMULATION OF THE PROBLEM

The problem is symmetric about the *x*-axis. Figure 1 shows the domain of interest in $-50 \le x \le 150$ and $0 \le y \le 50$, with an acoustic source centered at $x = 0$ and $y = 0$. The mean flow is parallel to the *x*-axis and the mean flow velocities, density and pressure are given by

$$\begin{cases} \bar{u}(y) = \begin{cases} u_j \exp\left[-(\ln 2)(y/b - h/b)^2\right] & y \ge h \\ u_j & 0 \le y \le h \end{cases} \\ \bar{v} \equiv 0 \\ \dfrac{1}{\bar{\rho}(y)} = -\dfrac{1}{2}\dfrac{\gamma-1}{\gamma\bar{p}}(\bar{u}(y)-u_j)\bar{u}(y) + \dfrac{1}{\rho_j}\dfrac{\bar{u}(y)}{u_j} + \dfrac{1}{\rho_\infty}\dfrac{u_j-\bar{u}(y)}{u_j} \\ \bar{p} = \text{constant} = 103330 \text{ m}^{-1}\text{ kg s}^{-2} \end{cases} \quad (1)$$

The governing equations are the two-dimensional linearized Euler equations (LEE) for a parallel mean flow in the *x*-direction.

$$\left(\frac{\partial}{\partial t} + A\frac{\partial}{\partial x} + B\frac{\partial}{\partial y}\right)\mathbf{U} + D\frac{\partial \bar{\mathbf{U}}}{\partial y} = \mathbf{S} \quad (2)$$

where

---

* Graduate research assistant
¶ Undergraduate summer research intern
§ Associate Professor

$$\mathbf{U}=\begin{bmatrix}\rho\\u\\v\\p\end{bmatrix}, A=\begin{bmatrix}\overline{u}&\overline{\rho}&0&0\\0&\overline{u}&0&1/\overline{\rho}\\0&0&\overline{u}&0\\0&\gamma\overline{p}&0&\overline{u}\end{bmatrix}, B=\begin{bmatrix}0&0&\overline{\rho}&0\\0&0&0&0\\0&0&0&1/\overline{\rho}\\0&0&\gamma\overline{p}&0\end{bmatrix}, \overline{\mathbf{U}}=\begin{bmatrix}\overline{\rho}\\\overline{u}\\\overline{v}\\\overline{p}\end{bmatrix}, D=\begin{bmatrix}v&0&0&0\\0&v&0&0\\0&0&0&0\\0&0&0&0\end{bmatrix},$$

$$\mathbf{S}=\begin{bmatrix}0\\0\\0\\A\exp\left[-\left(B_x x^2+B_y y^2\right)\right]\cos(\omega_o t)\end{bmatrix}$$

The non-homogeneous term $\mathbf{S}$ on the right hand side of equation (2) acts as the source term.

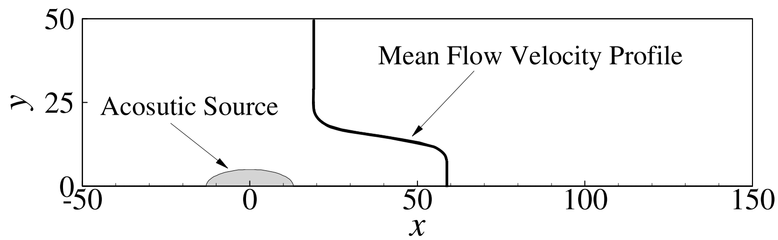

Figure 1. The domain of interest with an acoustic source centered at $x = 0$ and $y = 0$ and the schematic mean flow velocity profile.

The parameters for the problem are given in Table 1, where $M_j = u_j/a_j$ and $a_j = \sqrt{\gamma RT_j}$.

Table 1. The parameters used in the problem.

M_j	T_j (K)	T_∞ (K)	R ($m^2s^{-2}K^{-1}$)	γ	h (m)	b (m)	A (Kg m^{-1} s^{-3})	B_x (m^{-2})	B_y (m^{-2})	ω_o (rad s^{-1})
0.756	600	300	287.0	1.4	0.0	1.3	0.001	0.04ln(2)	0.32ln(2)	76

As we will see in the next section, the acoustic source at excitation frequency $\omega_o = 76$ rad/s will trigger a wave that grows along the *x*-direction and co-exists with the acoustic wave radiated from the acoustic source. Such a growing wave, termed as an instability wave, can overwhelm the acoustic wave solution where it is strong. Therefore, it is the requirement of the benchmark problem that the instability wave be "filtered out" to get the acoustic wave.

3. INSTABILITY WAVE AND ANALYTICAL SOLUTION

Instability wave

Assuming that the flow variables have a time- and space-dependence of the following form

$$\begin{cases}\rho=\Phi(y)e^{i(kx-\omega t)}\\u=U(y)e^{i(kx-\omega t)}\\v=V(y)e^{i(kx-\omega t)}\\p=P(y)e^{i(kx-\omega t)}\end{cases}\tag{3}$$

where k is the wavenumber in the *x*-direction, we can get the characteristic equation of the homogeneous LEE

$$\frac{d}{dy}\left(\frac{1}{\overline{\rho}(\omega-k\overline{u})^2}\frac{dP}{dy}\right)+\left(\frac{1}{\gamma\overline{p}}-\frac{k^2}{\overline{\rho}(\omega-k\overline{u})^2}\right)P=0\tag{4}$$

which is an ordinary differential equation (ODE) with only one unknown function $P(y)$.

The boundary condition at $y = 0$ is given by the symmetry condition

$$\frac{dP}{dy} = 0, \; y = 0 \tag{5}$$

In the far field, the medium is uniform, effectively free of acoustic source and without mean flow. Therefore, for a wavenumber k and an excitation frequency ω, the wave solution to equation (4) in that region must be in a form of $C\exp(i\beta y)$, where C is an arbitrary constant, $\beta = \sqrt{(\omega / a_\infty)^2 - k^2}$ and a_∞ is the sound speed in the far field. Note that a positive sign has been chosen for β such that the wave is outgoing at $y \to \infty$. When an equivalent form is used to get rid of the constant C, the boundary condition at $y \to \infty$ is

$$\frac{dP}{dy} = i\beta P, \; y \to \infty \tag{6}$$

The ODE (4) with its two boundary conditions (5) and (6) has a solution only for a certain wavenumber, or characteristic wavenumber, $k = \alpha$ for a given excitation frequency ω. Numerical procedures are implemented to find such an $\alpha - \omega$ relationship and the result is shown in Figure (2). At the excitation frequency given in the problem, $\omega = 76$ rad/s, the corresponding characteristic wavenumber is $\alpha = 0.4145 - 0.0377i$ (1/m), whose imaginary part is negative and thus the form assumed in equation (3) indicates a wave growing in the positive x-direction. Such a spatially amplifying wave is termed as an instability wave in this paper.

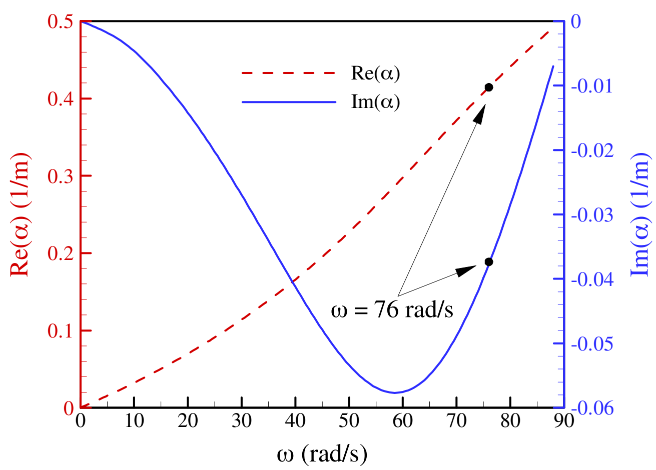

Figure 2. The characteristic wavenumber α for a given excitation frequency ω.

The above analysis shows that the instability wave is intrinsic to the homogenous system under the mean flow and boundary conditions given in section 2. It, therefore, exists in any non-homogeneous system that is obtained by adding acoustic source terms to the homogeneous system, as long as the homogenous system is linear. The non-homogenous term acts both as a source radiating acoustic waves to the surroundings and as a trigger to the instability wave.

Analytical solution to the acoustic wave

The analytical solution to such a problem has been derived by Dahl in a non-dimensional form by means of Fourier Transform and Green's functions (ref. 2). The solutions to the instability wave and the acoustic wave are obtained separately. Here we present only the derived formula for the acoustic pressure in a dimensional form.

$$p_a(k,y) = -\frac{iA^* M_j^2}{2\pi}\sqrt{\frac{\pi}{B'}}\int_{-\infty}^{\infty} e^{-k^2/4B'}\left[\zeta_1(k,y)\int_y^{\infty}\frac{\bar{\rho}(y_0)(\omega - \bar{u}(y_0)k)}{\Delta(k,y_0)}e^{-B'y_0^2}\zeta_2(k,y_0)dy_0 + \zeta_2(k,y)\int_0^{y}\frac{\bar{\rho}(y_0)(\omega - \bar{u}(y_0)k)}{\Delta(k,y_0)}e^{-B'y_0^2}\zeta_1(k,y_0)dy_0\right]dk \tag{7}$$

where $\zeta_1(k,y)$ ($\zeta_2(k,y)$) is the solution to the initial-value problem of the characteristic equation (3) only with the boundary condition at $y = 0$ ($y = \infty$) for a given wavenumber k; $\Delta(k,y)$ is the Wronskian of $\zeta_1(k,y)$ and $\zeta_2(k,y)$ with respect to y, defined as

$$\Delta(k, y) = \zeta_1(k, y)\frac{\partial \zeta_2(k, y)}{\partial y} - \zeta_2(k, y)\frac{\partial \zeta_1(k, y)}{\partial y} \tag{8}$$

Note that even $\zeta_1(k, y)$ and $\zeta_2(k, y)$, and thus their Wronskian, are not analytically obtainable for a general parallel mean flow condition. They, along with the integrals in equation (7) are numerically evaluated and the numerical result of the acoustic pressure will be compared with that of the numerical solution.

4. NUMERICAL SOLUTION

Numerical schemes

The problem is also numerically solved using a fourth-order seven-point-stencil optimized upwind Dispersion-Relation-Preserving scheme (ref. 3). The spatial coefficients for both the interior and the boundary points are the same as those listed in reference 3 while the temporal coefficients are from reference 4. The accuracy of this scheme has been demonstrated in reference 3.

One the left, right and upper boundaries, a radiation or absorbing boundary condition is to be applied to allow waves to leave the computational domain with minimum numerical reflections. In our problem, this requirement on such a boundary condition is made specially challenging due to two factors. One is the existence of the shear layer and the sharp change in its profile. The other is the exponentially amplifying effect of the instability wave, as has been seen in section 3. A weak wave generated by the numerical reflections could grow in the amplifying direction into one that is strong enough to contaminate the solution and the amplified wave will cause another reflected wave when hitting on the boundaries. We found that the Perfectly-Matched-Layer (PML) boundary condition in unsplit physical variables (ref. 5) can meet the requirement very satisfactorily. At the outer boundaries of the PML regions, a characteristics-based boundary condition is applied to terminate the computational domain. Note that a numerical implementation of the PML boundary condition in unsplit physical variables has not seen reported in a non-uniform mean flow condition, as in the current problem.

At the lower boundary of the domain of interest, a symmetry boundary condition is applied. A ghost point is introduced right below each of the node at the lower boundary in implementing the condition $\partial p/\partial y = 0$ at $y = 0$.

The domain of interest is uniformly discretized in the *x*-direction with grid spacing $\Delta x = 1.5$ m. In the *y*-direction, a clustered grid is used for a locally refined resolution of the shear layer and the source region. The grid density is specified as a function of the physical coordinate,

$$\left(\frac{dy}{d\xi}\right)_j = 1 - 0.6\exp[-(\ln 2)\ y_j^2/50] \tag{9}$$

where ξ is the transformed coordinate in the computational domain and j is the node index in the *y*-direction. Determined by equation (9), the size of the grid in the *y*-direction ranges from $\Delta y = 0.4$ m in the shear layer and the source region to $\Delta y = 1$ m in the far field. Shown in Figure 3 are the sizes and numbers of grid spacings used for the domain of interest and the PML region.

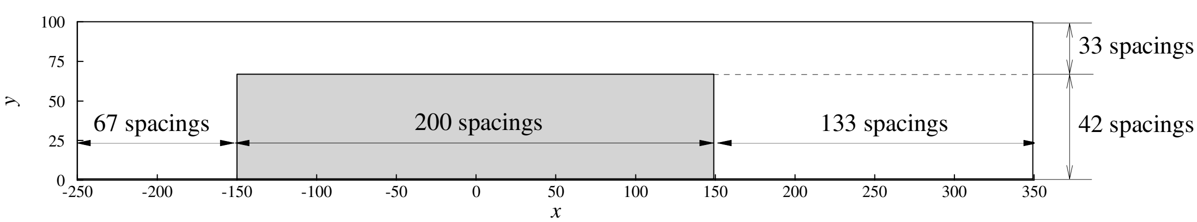

Figure 3. The whole computational domain with the PML region and the distribution of the grid spacings.

The time step is set to $\Delta t = 2.0668372\times10^{-5}s$, or a 4000th the period of the acoustic source at $\omega_0 = 76$ rad/s. A very periodic solution is reached after 200 periods, or 800,000 time steps. The CPU time and memory usage are about 7.5 hours and 10 MB on a computer with an Athlon XP 1800+ CPU at 1533MHz, 512MB physical memory and a compiler of DIGITAL Visual Fortran, version 6.0.A.

Shown in Figure 4 is the numerical solution for acoustic pressure *p* at the start of a period on the whole computational domain. The region outside the long-dashed-line rectangle is the PML region and the region confined by the short-dashed line is the domain of interest. We can see that the solution very distinctly consists of the acoustic waves radiated by the acoustic source centered at the origin and the instability wave growing along the *x*-direction.

Little reflection is observed at the interface of the interior and the PML region and both of the acoustic wave and the instability wave are absorbed very neatly in the PML region. In contrast to the analytical solution, where the instability wave and the acoustic wave are obtained separately, the numerical solution always gives the total solution, i.e., the sum of the two wave solutions. Therefore, we need to subtract the instability wave solution from the total solution to get the acoustic wave solution.

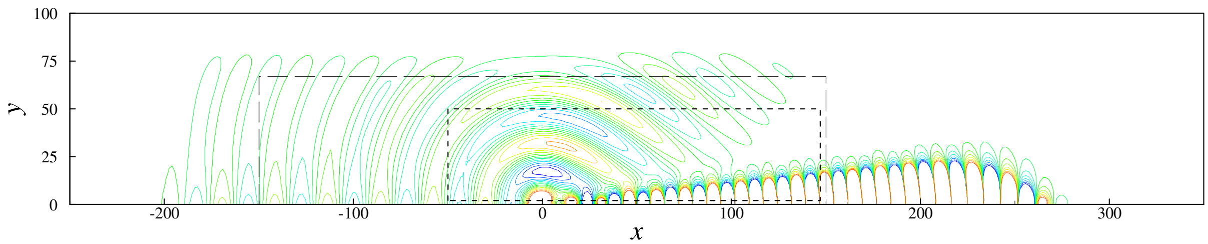

Figure 4. The acoustic pressure for the total solution at the start of a period in the whole computational domain of -250 ≤ x ≤ 350 and 0 ≤ y ≤ 100. Outside the region confined by the long-dashed line is the PML region; the region confined by the short-dashed line is the domain of interest.

Separation of the instability and acoustic waves

In order to get the instability wave solution, a source term of the same excitation frequency is effectively placed upstream of the region of interest (-50 ≤ x ≤ 150 and 0 ≤ y ≤ 50). Such a source term produces a stronger instability wave but a weaker acoustic wave in the region of interest and thus the total solution in this region can well approximate a pure instability wave. We use a dipole as such a source since the acoustic wave that it produces tends to be more local to the source. The numerical solution in such a configuration is calculated with the same numerical schemes on the same grid and is assumed to be a pure instability wave in the domain of interest. Since the instability wave is an eigen-solution of the homogeneous LEE, the instability waves in the two numerical solutions differ with a complex constant, or two real constants, corresponding to the phase and the amplitude. Thus we adjusted the phase and the amplitude of the "pure" instability wave to those of the total solution based on a grid point at $x = 147$ m and $y = 0$ m . We then get the acoustic wave solution by subtracting the adjusted instability wave solution for the total solution. Figures 5 (a), (b) and (c) show the acoustic pressure field at the start of a period in the region of interest for the total solution, the (adjusted) instability wave solution, and the acoustic wave solution respectively. Figures 6 (a), (b) and (c) show the pressure at the start of a period along the lines of -50 ≤ x ≤ 150 at y = 15, -50 ≤ x ≤ 150 at y = 50 and 5 ≤ y ≤ 50 at x = 100, as compared with the analytical solution calculated in section 2. The agreements between the numerical solutions and the analytical solutions are excellent.

5. CONCLUSIONS AND DISCUSSIONS

In this paper, we demonstrate a numerical method to calculate and separate the acoustic wave and the instability wave in a two-dimensional shear layer. The method is entirely based on the time domain calculations and is verified by the analytical solution to the same problem. To exploit the advantage of time-domain methods, it is desirable to extend the current method to the cases of multi-frequency and broadband sound sources.

6. REFERENCES

1. Morris, Phillip J.; Agarwal, Anurag: “Radiation and Refraction of Sound Waves through a Two-Dimensional Shear Layer,” the Fourth Computational Aeroacoustics Workshop on Benchmark Problems, Cleveland, Ohio, October, 2003.
2. Dahl, Milo D.: "Solution to the Category 5 Problem: Generation and Radiation of Acoustic Waves from a 2D Shear Layer," *Proceedings of the Third Computational Aeroacoustics Workshop on Benchmark Problems*, Cleveland, Ohio, November, 1999, NASA/CP-2000-209790, August, 2000, pp. 87-92.
3. Zhuang, M.; Chen, R. F.: “Applications of High-Order Optimized Upwind Schemes for Computational Aeroacoustics,” *AIAA Journal*, Vol. 40, No. 2, 2002, pp. 443-449.
4. Tam, C. K. W.; Webb, J. C.: “Dispersion-Relation-Preserving Finite Difference Schemes for Computational Acoustics,” *Journal of Computational Physics*, Vol. 107, No. 2, 1993, pp. 262-281.

5. Hu, F. Q.: “A Stable, Perfectly Matched Layer for Linearized Euler Equations in Unsplit Physical Variables,” *Journal of Computational Physics*, Vol. 173, 2001, pp. 455-480.

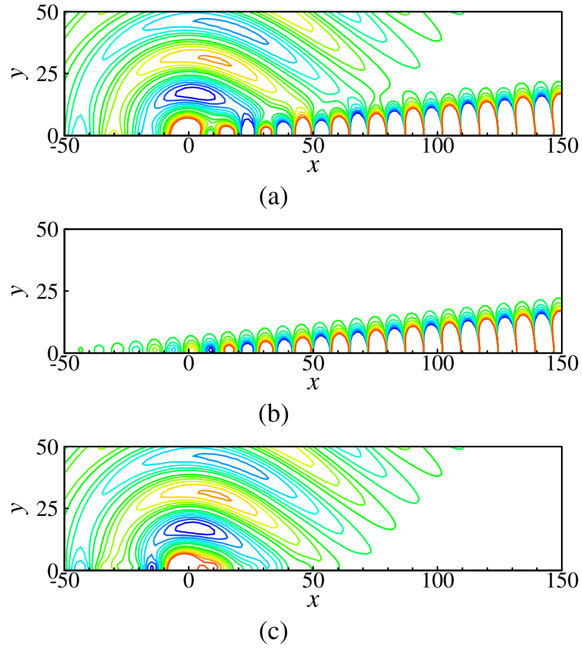

Figure 5. The acoustic pressure at the start of a cycle in the domain of interest. (a) the total solution; (b) the (adjusted) instability wave solution; (c) the acoustic wave solution.

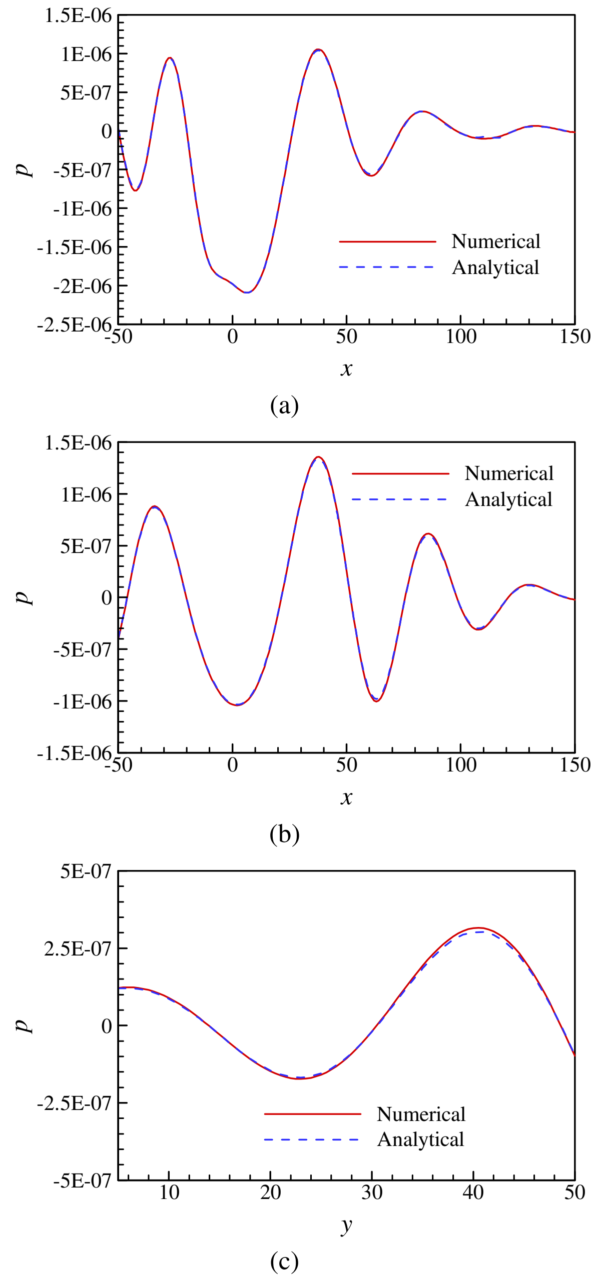

Figure 6. The acoustic pressure at the start of a cycle as compared with the analytical solution along the lines of (a) $-50 \le x \le 150$ at $y = 15$, (b) $-50 \le x \le 150$ at $y = 50$, and (c) $5 \le y \le 50$ at $x = 100$.